Efficient Phenomenologically-based 1-D Evaluation of the Impedance Matrix in a MPIE Analysis of Planar Microstrip Circuits

F. Cervelli, M. Mongiardo, L. Tarricone

Istituto di Elettronica
Via G. Duranti, 93, 06131, Perugia, Italy.

I. Abstract

The analysis of microstrip circuits via integral equation techniques has proven as the most efficient, and yet rigorous and full-wave, approach. Nonetheless, the latter requires the evaluation of the impedance matrix which elements, in turn, are generally obtained after a two-dimensional numerical integration.

We introduce a coordinate transformation allowing to reduce, for the mixed potential integral equation, the numerical integration to a one-dimensional case. Moreover, by using the spatial domain closed-form of the Green's function and by phenomenologically separating the relevant contributions, we demonstrate that a significant reduction of computer times is indeed feasible and achievable.

II. Introduction

The efficient evaluation of the impedance matrix $\mathbf{Z}$ of a planar circuit is a crucial issue for achieving accurate and fast analyses. The $\mathbf{Z}$ computation, as attained by Method of Moments (MoM) discretization of the Mixed-Potential Integral Equation (MPIE) [1], [2], in fact, is not entirely straightforward, and the related numerical efforts are still considerable.

In previous approaches, the numerical core of the computation of the impedance matrix was represented by a time-demanding two-dimensional integration, even though several efforts have been made to improve the convergence of this computation [3], [4]. Some attempts in this sense have also been made focussing on appropriate choices of the basis and test functions [5], with attention paid on the meshing performed on the problem's domain.

In this paper, a substantial enhancement of the efficiency of the impedance matrix evaluation is achieved by reducing the two-dimensional integration to a single-dimension one. Even though this is achieved by partitioning the problem domain into equal cells, this does not represent a limitation to the presented technique, as different optimum sizes for the elementary cells can be automatically detected in several regions of a single circuit, so that an optimum accuracy is ensured.

Moreover, a detailed study on the phenomenological behaviour of the impedance matrix elements is performed, and its conclusions implemented so that substantial speed-ups are achieved.

III. Z-Matrix Evaluation

Let us denote with $\mathbf{E^s}$ the scattered electric field, with $\mathbf{Z_s}$ and $\mathbf{J_S}$ the surface impedance and electric current density, respectively, and let us introduce the Green's functions $\bar{\bar{\mathbf{G}}}^{\mathbf{A}}$ and G^q for the surface electric current density $\mathbf{J_S}$ and for the surface electric charge density q_S. With the above notation the standard MPIE is written as:

$$\mathbf{n} \times \mathbf{E^e}(\mathbf{r}) = \mathbf{n} \times (\mathbf{Z_S J_S} - \mathbf{j}\omega \int_{\mathbf{S}} \bar{\bar{\mathbf{G}}}^{\mathbf{A}} \cdot \mathbf{J_S}\, \mathbf{dS'} + \nabla \int_S G^q \cdot q_S\, dS') \tag{1}$$

Closed-form Green's functions can be used [6], [7], [8], expressed as the sum of three main contributions:

- direct terms and quasi-dynamic images;
- surface waves;
- complex images;

0-7803-4471-5/98/$10.00 (c) 1998 IEEE

so that we can write them as:

$$G^A_{xx} = G^A_{xx,0} + G^A_{xx,SW} + G^A_{xx,ci}$$
$$G^q = G^q_0 + G^q_{SW} + G^q_{ci} \tag{2}$$

Equation (1) is discretized and solved using the Galerkin's MoM, producing a linear system

$$\begin{bmatrix} Z_{xx} & Z_{xy} \\ Z_{yx} & Z_{yy} \end{bmatrix} \begin{bmatrix} I_x \\ Iy \end{bmatrix} = \begin{bmatrix} V_x \\ Vy \end{bmatrix} \tag{3}$$

A. Efficient Evaluation Via 1-D Integration

The entries Z_{ij} in the impedance matrix represent the tangential electric field generated by the j-th basis function and weighted by the i-th test one. In previous approaches [5], the entries of the matrix in (3) are expressed as a four-dimensional integral:

$$< f, G * g >= \int\int f(x,y) \int\int G(r) g(x,y)\, dx'dy'dxdy \tag{4}$$

$r = \sqrt{(x-x')^2 + (y-y')^2}$, and the four-fold integration appearing in (4) is therein transformed into a two-dimensional one. In this contribution, we show how the latter integration can be reduced to a one-dimensional integral.

The usual change of variables,

$$\begin{aligned} x - x' &= u & x + x' &= p \\ y - y' &= v & y + y' &= q \end{aligned} \tag{5}$$

reduces the problem to a double integration, hence providing

$$\int\int f(x,y) \int\int G\left(\sqrt{(x-x')^2 + (y-y')^2}\right)$$
$$g(x',y')\, dx'\, dy'\, dx\, dy = \frac{1}{4} \int\int G(u,v)$$
$$\int\int f\left(\frac{u+p}{2}, \frac{v+q}{2}\right) g\left(\frac{p-u}{2}, \frac{q-v}{2}\right) dp\, dq\, du\, dv$$

Letting D_x be the domain for the x-variable, we can write

$$S(u,v) \triangleq \frac{1}{4} \int_{D(p)} \int_{D(q)} f\left(\frac{u+p}{2}, \frac{v+q}{2}\right) g$$
$$\left(\frac{p-u}{2}, \frac{q-v}{2}\right) dp\, dq = \tag{6}$$
$$= \int_{D(\zeta)} \int_{D(\eta)} f(\zeta,\eta) g(\zeta - u, \eta - v)\, d\zeta\, d\eta$$

Now we have a two-variable integration

$$\int_{D(u)} \int_{D(v)} G(u,v) S(u,v)\, du\, dv \tag{7}$$

With the following new change of variables:

$$u = r\cos\xi \qquad v = r\sin\xi \tag{8}$$

we can write:

$$\int_{D(u)} \int_{D(v)} G(u,v) S(u,v)\, du\, dv =$$
$$= \int_{r_1}^{r_2} G(r) r \int_{\xi_1(r)}^{\xi_2(r)} S(r\cos\xi, r\sin\xi)\, d\xi\, dr \tag{9}$$

Thanks to the fact that the Green's functions only depend on the source-test distance r, W(r) can be evaluated in closed form:

$$W(r) \triangleq \int_{\xi_1(r)}^{\xi_2(r)} S(r\cos\xi, r\sin\xi)\, d\xi \tag{10}$$

Finally we have:

$$\int\int f(x,y) \int\int G(\sqrt{(x-x')^2 + (y-y')^2})$$
$$g(x',y')\, dx'\, dy'\, dx\, dy = \tag{11}$$
$$= \int_{r_1}^{r_2} W(r) G(r) r\, dr$$

Using polar coordinates Green's functions are not singular, and with a suitable choice [5] of basis and test functions $W(r)$ is integrable in Riemann sense. The $S(u,v)$ and $W(r)$, as well as the forms of domains $D(p)$ and $D(q)$, $\xi_1(r)$ and $\xi_2(r)$, r_1 and r_2, depend on the choice of the basis and test functions and their domain of definition.

After evaluating $W(r)$, the Z-matrix terms can be written as:

$$Z_{xx} = \int \left[W_{1x}(r) G^A_{xx}(r) - \frac{1}{\omega^2} W_{2x}(r) G^q(r)\right] r\, dr$$
$$Z_{xy} = \int \left[-\frac{1}{\omega^2} W_{3x}(r) G^q(r)\right] r\, dr$$
$$Z_{yx} = \int \left[-\frac{1}{\omega^2} W_{3y}(r) G^q(r)\right] r\, dr \tag{12}$$
$$Z_{yy} = \int \left[W_{1y}(r) G^A_{yy}(r) - \frac{1}{\omega^2} W_{2y}(r) G^q(r)\right] r\, dr$$

thus demonstrating that the elements of the impedance matrix can be evaluated by solving a one-dimensional integral.

B. Results with 1-D Integration

The accuracy and efficiency of the implemented method is demonstrated for a patch antenna, reported in the literature [7], and sketched in Fig. 1. In Fig. 2 we compare the time performance of an MPIE/MoM package implementing a 1-D integration of the (4) with respect to the previous 2-D integration proposed by [5]. In the x-axis the required numerical accuracy is reported, on the y-axis the corresponding computing time for both approaches. As easily predictable, the 1-D integration is highly superior. From the circuit schematic in Fig. 1, it is also apparent that the requirement of an equal-cell meshing is not limiting, as suitable sizes of elementary cells for the different regions of a complex circuit can automatically be detected with simple heuristic considerations.

IV. Phenomenological Behaviour of the Z-Matrix Elements

The 1-D integration significantly reduces the computation time of the impedance matrix. In addition, further advantage can be attained by considering the behaviour of the integration kernels in (12). A major role in the numerical evaluation of (12), is played by the Green's function; its expression as reported in (2) separates the contribution of different physical phenomena (quasi-static, surface waves and complex images) in the interactions among cells.

Therefore, by considering each element of the **Z** matrix as the sum of the three above mentioned contributions, a phenomenological analysis has been performed in order to investigate how these contributions are linked with the circuit physical parameters. Referring to the circuit in Fig. 1, results are sketched in Table I, where, for the sake of conciseness, we report just some of the available results. It can be observed that for each element of the impedance matrix, the three Green's function's contributions are separated, and a number of cells along x and y directions determined, so that the corresponding contribution can be neglected for distances between basis and test greater than that number of cells. For instance, we understand from Table I that the basis-test interaction for the quasi-static term Z_{xxo} is effective for distances smaller than 11 cells along x, and 9 cells along y, as well as the surface wave contribution can be nearly neglected. We consider negligeable each interaction smaller than $10^{-5} Z_{xx}(0,0)_o$, where $Z_{xx}(0,0)_o$ is the direct-term evaluated in the (0,0) cell (the same term is the maximum entry in the impedance matrix).

Z element	*x-cells*	*y-cells*
Z_{xxo}	11	9
Z_{xxsw}	1	2
Z_{xxci}	7	6
Z_{xyo}	6	6
Z_{xysw}	0	0
Z_{xyci}	7	6

Table I

A. Results Achieved by Exploiting the Phenomenological Analysis

The phenomenological analysis has demonstrated that, for a fixed threshold, some contributions in the integration kernels in (12) can be omitted, with a consequent enhancement in the code performance. Moreover, and of much higher impact, we can avoid the computation of many interacting terms, which prove to be nearly negligeable. In fact, the use of the above mentioned 10^{-5} threshold affects the final results with a maximum error of less than 1%.

The implementation of the results of the phenomenological analysis allows a huge speed-up. Referring to the circuit in Fig. 1, in Table II the use of a traditional approach is compared with our approach, implementing a 1-D integration technique and a phenomenological analysis. Times (in seconds) refer to the evaluation of the Z-matrix for a single frequency point. An IBM RS6000 250 T has been used.

Method	*Computing Time*
Standard	2040
With 1-D Int.	411
With 1-D Int.+ Phen. An.	86

Table II

V. Conclusion

In this paper we have introduced a procedure for evaluating the elements of the impedance matrix, as resulting from the mixed-potential integral equation, via a single one-dimensional numerical integration.

Moreover, we have also shown that it is possible to take advantage of the fact that the direct term, the surface waves and the complex images appearing in the spatial domain closed-form Green's function play different roles according to the problem geometrical parametrization. Hence, depending on the respective positions of basis and test functions, we can neglect some contributions without loss of accuracy and with significant reduction of the numerical burden. Speed-ups of more than 22 times have been observed, with respect to the previous state-of-the art implementations of the same approach.

REFERENCES

[1] J. R. Mosig and F. E. Gardiol, "General integral equation formulation for microstrip antennas and scatterers", *Proc. Inst. Elec. Eng., pt. H: Microwave Optics Antennas*, vol. 132: pp. 424–432, Dec. 1985.

[2] J. R. Mosig, "Arbitrarly shaped microstrip structures and their analysis with a mixed potential integral equation", *IEEE Trans. Microwave Theory Tech.*, vol. 36: pp. 314–323, Feb. 1988.

[3] L. Barlatey, J. R. Mosig and T. Sphicopoulos, "Analysis of stacked microstrip patches with a mixed potential integral equation", *IEEE Trans. Microwave Theory Tech.*, vol. 38: pp. 608–615, May 1990.

[4] M. I. Aksun and R. Mittra, "Estimation of spurious radiation from microstrip etches using closed-form Green's functions", *IEEE Trans. Microwave Theory Tech.*, vol. 40: pp. 2063–2070, Nov. 1992.

[5] M. I. Aksun and R. Mittra, "Choices of expansion and testing functions for the method of moments applied to a class of electromagnetic problems", *IEEE Trans. Microwave Theory Tech.*, vol. 41: pp. 503–508, Mar. 1993.

[6] M. I. Aksun and R. Mittra, "Derivation of closed-form Green's functions for a general microstrip geometry", *IEEE Trans. Microwave Theory Tech.*, vol. 40: pp. 2055–2062, Nov. 1992.

[7] G. Dural and M. I. Aksun, "Closed-form Green's functions for general sources and stratified media", *IEEE Trans. Microwave Theory Tech.*, vol. 43: pp. 1545–1552, Jul. 1995.

[8] N. Kynaiman and M. I. Aksun, "Efficient and Accurate EM Simulation Technique for Analysis and Design of MMICs", *Int. J. MW and MM Wave Comp. Aided Eng.*, vol. 37: pp. 344–358, Sept. 1997.

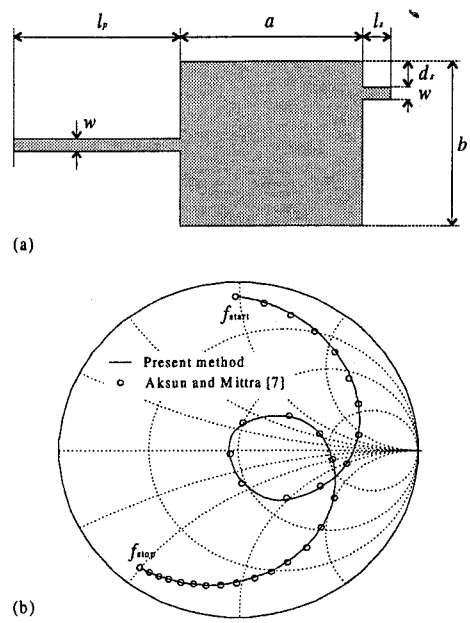

Fig. 1. Input impedance on the Smith chart (b) of the microstrip line center fed square antenna with a tuning stub (a). Physical dimensions: $\epsilon_r = 2.62$, d = 0.794 mm, a = b = 28.6 mm, w = 2.2 mm, l_p = 26.4 mm, l_s = 4.4 mm, d_s = 4.4 mm. Frequency range: 2.98-3.3 GHz.

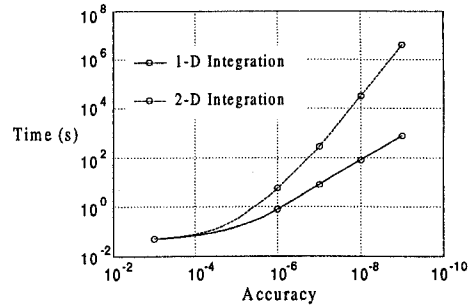

Fig. 2. A comparison between the 1-D and the 2-D integration's performance. Times refer to a PC Pentium 100 MHz. On the x-axis, the accuracy required to make the integration converge is reported.